EVIDENCE OF DEPOSITIONAL SETTINGS VARIATION AT THE JURA/KNOCKFARRIL HILL MEMBERS TRANSITION IN THE GLEN TORRIDON REGION (GALE CRATER, MARS). G. Caravaca[1*], N. Mangold[1], E. Dehouck[2], J. Schieber[3], A.B. Bryk[4], C.M. Fedo[5], S. Le Mouélic[1], S.G. Banham[6], S. Gupta[6], A. Cousin[7], W. Rapin[7], O. Gasnault[7], R.C. Wiens[8]. [1]UMR CNRS 6112 LPG, Univ. Nantes, France, [2]LGL-TPE, Univ. Lyon, France, [3]Indiana University, IN, [4]University of California, Berkeley, CA, [5]Dept Earth & Planetary Sciences, University of Tennessee, Knoxville, TN, [6]Imperial College London, UK, [7]IRAP, Toulouse, France, [8]LANL, Los Alamos, NM. *gwenael.caravaca@univ-nantes.fr.

Introduction: Since Jan. 2019 (~sol 2300), the Mars Science Laboratory rover *Curiosity* has been exploring the Glen Torridon (GT) region of Gale Crater, seeking to examine clay-bearing strata initially detected using orbiter data [1]. The presence of hydrated clay minerals has major implications for understanding the wet early Mars. The sedimentary record of the GT region is comprised of mudstones interbedded with very fine- to medium-grained sandstones of the Jura and Knockfarril Hill (KHm) members of the Murray Fm., respectively [2]. However, their varying sedimentary, stratigraphic, and geochemical characteristics suggest potential changes in the depositional settings that could have favored enhanced accumulation and/or *in situ* formation of secondary clay minerals [e.g., 3]. Here, we examine the sedimentary and geochemical records of four major outcrops (Woodland Bay, Teal Ridge, Strathdon area and Glen Etive) in the northern part of GT, an area where exceptionally developed outcrops are present.

Dataset: Four Digital Outcrop Models (DOM) were computed using Structure-from-Motion photogrammetry based on Navcam, Mastcam and MAHLI imagery from the rover [4, 5]. These models allow 3D and multi-scale characterization of sedimentary features in each outcrop, and permit reconstruction of stratigraphic relationships between the members [5]. MAHLI and ChemCam's RMI images were used to determine texture and grain-size. In addition, 40 targets were analyzed using the ChemCam instrument to provide quantification of major rock-forming oxides using Laser-Induced Breakdown Spectroscopy [6].

Facies analysis: Two main facies are observed in this area. Facies A is characterized by a fine-grained texture (from mudstone to fine sandstone) and crops out as cm-scale beds where faint planar parallel laminations can be occasionally identified (A in Fig. 1). It is less resistant to erosion (fragmented in Fig. 1a, recessive in Fig. 1b). This facies is interpreted to represent low energy conditions commonly encountered in lake deposits (i.e., deposition from suspension), and comparable with characteristics of the main type of facies in the underlying Jura member [7]. Facies B is characterized by coarser-grained (fine to medium) sandstones and shows cross-stratifications with bedsets at the cm- to dm-scale (B in Fig. 1). It is more erosion resistant (Fig. 1b) and forms prominent meter-scale mesas-like outcrops. This facies represents deposition under higher energy, but with differing characteristics from cross-stratified sandstones previously observed in the Murray Fm. at Pahrump Hills [8], more likely suggesting a lake-shore to fluvial environment, that persists into the KHm.

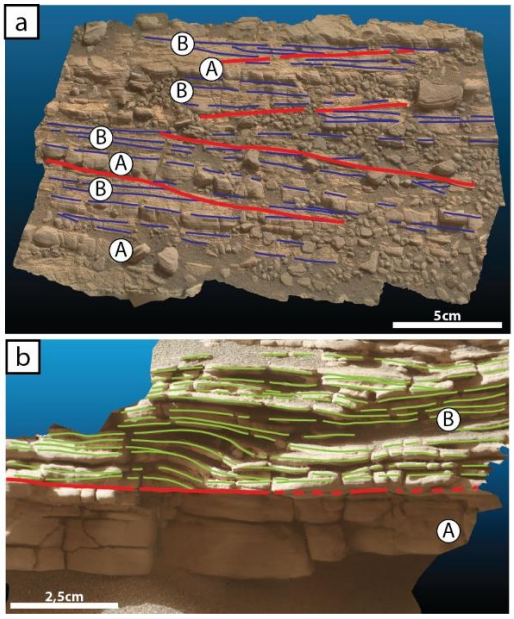

Fig. 1 a) Interpreted DOM of the Morningside target (sol 2424, Woodland Bay outcrop), highlighting interfingering of facies A mudstones with facies B sandstones, the latter showing small-scale cross-stratification (blue lines) and truncations (red lines); b) Interpreted DOM of the Strathdon target (sol 2462), highlighting cross-stratified (green lines) facies B lying unconformably upon facies A (red line).

Geometric relationships between facies: Two types of stratigraphic relationships are observed between facies A and B. First, a progressive transition is notably seen on the Morningside target (Fig. 1a), showing alternations and interfingering between facies A and B (left on Fig. 2). Second, a sharp, erosional contact between A and B is observed, such as on the Strathdon target (Fig. 1b, right on Fig. 2). These differences high-

light both lateral and vertical variations in the local depositional settings through the transition up-section from lacustrine conditions (Jura member, dominated by facies A) and toward more energetic conditions of lake-shore to fluvial settings (KHm, dominated by facies B).

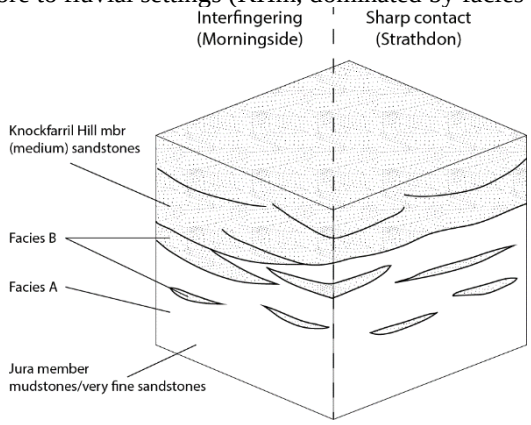

Fig. 2 Representation of co-occurring interfingering (left) and sharp (right) transitions observed between the facies A and B, indicating lateral and vertical variations in the depositional settings.

Geochemical data: Investigations of the GT area by the ChemCam LIBS and APXS instruments led to the distinction of two major compositional end-members mainly discriminated by their MgO and K_2O contents and named after the apparent morphology of the targets [3, 9, 10]. The "rubbly" end-member shows a composition enriched in K_2O (>1.5wt.%) and depleted in MgO (usually <6wt.%), whereas the "coherent" end-member shows MgO enrichments (~6 to 11wt.%). The co-occurrence of such end-members in close range is unusual when compared to the rest of the Murray Fm. [9]. Fig. 3 demonstrates that facies A and B can also be discriminated based on these two oxides.

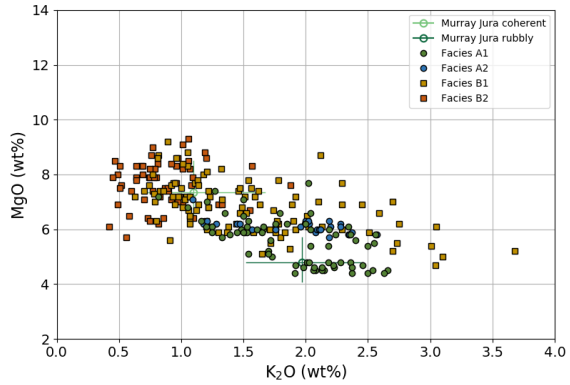

Fig. 3 Major-oxide composition of GT samples showing a geochemical distinction in MgO and K_2O compositions between facies A and B, in accordance with the "rubbly" *vs* "coherent" end-members distinction. Each point represents a single analysis point.

Indeed, facies A targets show an enrichment in K_2O (~1 to 2.7wt.%) and a depletion in MgO, whereas facies B targets show an enrichment in MgO (~6 to 9.5wt.%) and a variable but generally lower K_2O content. Thus, facies A is broadly in line with the "rubbly" end-member, and facies B with the "coherent" end-member. This correlation between the sedimentological and geochemical signals of the rocks raises the question of the role of the changing depositional settings in segregating the geochemical and/or mineralogical species [see also 9], but also of possible varying sources of the sedimentary material [see also 3].

Summary: We observe in the northern part of GT a transition in the depositional settings, evidenced in both the sedimentary and geochemical records. This transition reflects a shift from a low energy deposition in a lacustrine environment expressed by the fine-grained Jura member (and the overall underlying Murray formation [2, 7]), towards more energetic fluvial-influenced conditions represented by the cross-stratified sandstones of the KHm. This transition is characterized by rapid lateral and vertical variations of the depositional settings evidenced by the presence of both progressive (with interfingering) and sharp, erosional contacts between the two members. Also, the geochemical affinity of the facies B sandstones with the "coherent" end-member (notably in alkali elements) shows that KHm-like sandstones occur lower than previously described, even interfingering with the Jura member mudstones. Further investigations will try to settle whether those depositional settings changes are responsible for the variations in abundance and types of clay minerals present in GT [see also 3, 9]. Finally, as the rover continues to climb up section, it will be important to test whether the paleoenvironmental change recorded at the Jura/KHm transition is restricted to GT or part of a broader evolution ("continentalization") of the depositional settings in a drying Gale crater, as hinted by possibly aeolian deposits observed in the overlying "sulfate unit" [11].

References: [1] Milliken, R.E. et al. (2010) *Geophys Res Lett, 3, L04201*. [2] Fedo, C.M. et al. (2020) *LPSC LI* Abstract #2345. [3] Cousin et al. (2021) *LPSC LII* (this conf.). [4] Caravaca, G. et al. (2020) *Planet Space Sci.*, 182, 104808 [5] Caravaca, G. et al. (2020) *EPSC Abstracts*, 14, EPSC2020-49.[6] Clegg S. M. et al. (2017) *Spectrochim. Acta B*, 129. [7] Edgar et al. (2020) *JGR Planets*, 125, e2019JE006307. [8] Stack et al. (2019) *Sedimentology* 66, 1768–1802. [9] Dehouck et al. (2019) *Mars 9* Abstract #6125. [10] O'Connell-Cooper et al. (2020) *LPSC LI* Abstract #2948. [11] Rapin et al. (2021) *LPSC LII* (this conf.)